Biometals (2017) 30:321–334
DOI 10.1007/s10534-017-0008-z

Human topoisomerase inhibition and DNA/BSA binding of Ru(II)–SCAR complexes as potential anticancer candidates for oral application

Rone A. De Grandis · Mariana S. de Camargo · Monize M. da Silva · Érica O. Lopes · Elias C. Padilha · Flávia A. Resende · Rosângela G. Peccinini · Fernando R. Pavan · Alessandro Desideri · Alzir A. Batista · Eliana A. Varanda

Received: 18 January 2017 / Accepted: 7 March 2017 / Published online: 16 March 2017

Abstract Three ruthenium(II) phosphine/diimine/picolinate complexes were selected aimed at investigating anticancer activity against several cancer cell lines and the capacity of inhibiting the supercoiled DNA relaxation mediated by human topoisomerase IB (Top 1). The structure–lipophilicity relationship in membrane permeability using the Caco-2 cells have also been evaluated in this study. **SCAR 5** was found to present 45 times more cytotoxicity against breast cancer cell when compared to cisplatin. **SCAR 4** and **5** were both found to be capable of inhibiting the supercoiled DNA relaxation mediated by Top 1. Interaction studies showed that **SCAR 4** and **5** can bind to DNA through electrostatic interactions while **SCAR 6** is able to bind covalently to DNA. The complexes **SCAR** were found to interact differently with bovine serum albumin (BSA) suggesting hydrophobic interactions with albumin. The permeability of all complexes was seen to be dependent on their lipophilicity. **SCAR 4** and **5** exhibited high membrane permeability ($P_{app} > 10 \times 10^{-6}$ cm·s^{-1}) in the presence of BSA. The complexes may pass through Caco-2 monolayer via passive diffusion mechanism and our results suggest that lipophilicity and interaction with BSA may influence the complexes permeation. In conclusion, we demonstrated that complexes have powerful pharmacological activity, with different results for each complex depending on the combination of their ligands.

R. A. De Grandis (✉) · É. O. Lopes · E. C. Padilha · R. G. Peccinini · F. R. Pavan · E. A. Varanda
School of Pharmaceutical Sciences, São Paulo State University, Araraquara 14800-903, Brazil
e-mail: degrandis.rone@usp.br

M. S. de Camargo · M. M. da Silva · A. A. Batista
Center of Exact Sciences and Technology, Federal University of São Carlos, São Carlos 13565-905, Brazil

F. A. Resende (✉)
Department of Health and Biological Sciences, University of Araraquara, Araraquara 14801-340, Brazil
e-mail: flaviabiomed@yahoo.com.br

A. Desideri
Department of Biology, University of Rome Tor Vergata, Rome 173, Italy

Graphical Abstract

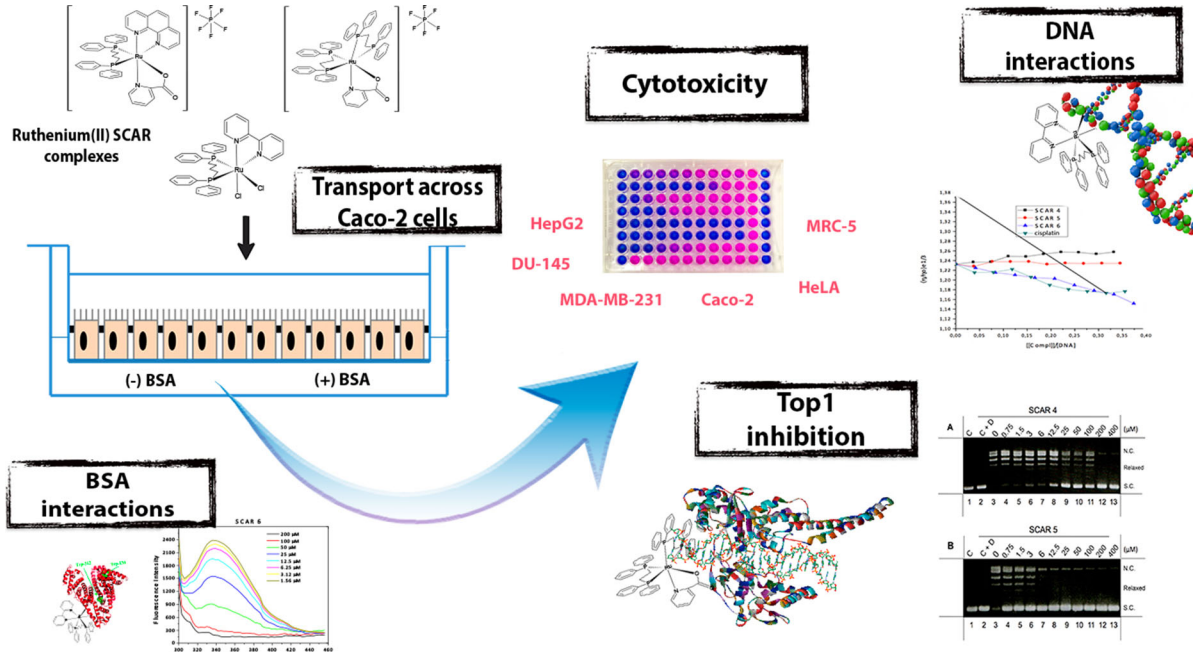

Keywords Anticancer agent · Ruthenium(II) complexes · Topoisomerase · Binding affinity · Caco-2 permeability

Introduction

The research based on metallopharmaceuticals was strongly encouraged thanks to the quest for anticancer therapies aiming at replacing platinum-based drugs with other (less toxic) cytotoxic agents. Ruthenium complexes occupy an important place in the field of medicinal inorganic chemistry due to their unique chemical properties as low toxicity and a wide range of biological activities (Allardyce and Dyson 2001; Barton et al. 2011; Li et al. 2012; Messori et al. 2013; Corrêa et al. 2016). Many ruthenium complexes have undergone scrutiny for clinical applications, particularly in the treatment of cancer. Ruthenium(II) complexes have been attracting considerable interest as potential anticancer and anti-tuberculosis drugs (Page 2012; Pavan et al. 2013; Allardyce and Dyson 2016). Therefore, as part of our ongoing effort to design new bioactive metallodrug candidates, our research group has synthesized a number of ruthenium complexes with phosphine/diimine/picolinate ligands "**SCAR**" (acronym to São Carlos and Araraquara, the cities of our research group) which have shown promising activity in vitro, especially against tuberculosis (Pavan et al. 2011, 2013). **SCAR 4–6** (Fig. 1) were selected to evaluate their yet unknown anticancer activity once previous studies have shown significant results about their genotoxicity and selective mode of action on tumor cells (De Grandis et al. 2016).

Most anticancer agents are designed to act in cell proliferation, inhibiting DNA replication. Human DNA topoisomerase IB (Top 1) is primarily an essential enzyme that aids in solving topological problems associated with DNA replication and transcription (Roca 1995), and often overexpressed in cancerous cells (Barros et al. 2013). Oddly enough, while numerous reports have demonstrated the potential of ruthenium(II) complexes focusing on DNA interaction (Barton et al. 2011), albumin interaction (Nišavić et al. 2016) and cytotoxicity (Gou et al. 2015), their ability when it comes to the simultaneous inhibition of Top 1 activity has, nonetheless, been given very little attention. Recently, genotoxicity of **SCAR** complexes was elucidated, showing that the combination of phosphine/diimine/picolinate ligands may influence the responses of chromosomal breaks, indicating possible formation of adducts in DNA (De Grandis et al. 2016).

The next step in the development of anticancer candidates lies within the analysis of the processes

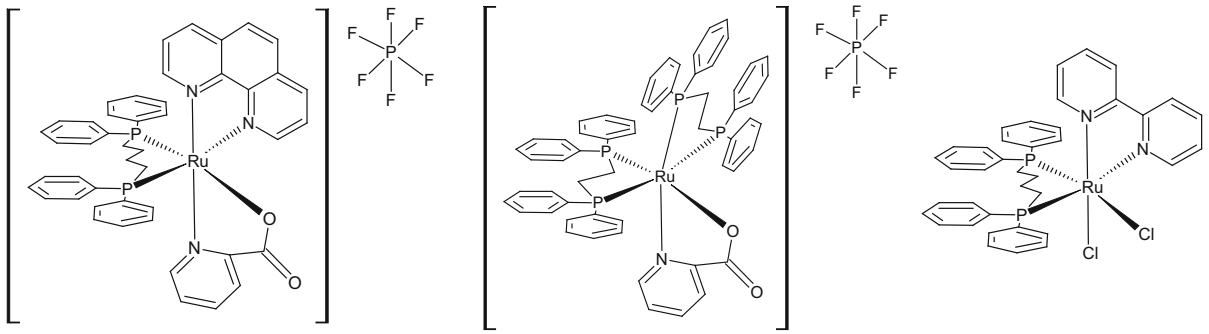

SCAR 4 **SCAR 5** **SCAR 6**

Fig. 1 Ruthenium(II) **SCAR** structures

involved in their pharmacokinetic profile. Interestingly, oral drug formulations of anticancer agents are increasingly being developed. The incentives for oral drug formulation of anticancer agents include improved safety, efficacy, quality of life, reduced cost, besides the ability to deliver chemotherapy at home and to apply drug schedules that maximize an agent's efficacy (Lu and Mahato 2009). A wide range of models based on cell cultures for the determination of the in vitro intestinal permeability have been developed. Among them, the Caco-2 cells, have been extensively employed. The predictive capability of drug absorption potential using Caco-2 cells has also been broadly demonstrated (Artursson et al. 2001; Stenberg et al. 2001; Hubatsch et al. 2007). Thus, the drug's apparent permeability (P_{app}) through these cells can be said to be a valuable parameter useful in estimating the uptake of orally administered drugs (Grès et al. 1998).

Admittedly, to date no reports are found in the literature vis-à-vis the influence exerted by lipophilicity, thanks to the phosphine/diimine/picolinate ligands, on the cytotoxicity and permeability of ruthenium(II) complexes. The vital need and importance of evaluating their permeability aiming at less invasive therapies that cause less social comorbidity to patients cannot, in the least bit, be over emphasized.

Materials and methods

Materials and solutions

Resazurin sodium salt (CAS 62758-13-8), bovine serum albumin (BSA, CAS 9048-46-8), calf-thymus DNA (ct-DNA, CAS 73049-39-5), dimethyl sulfoxide (DMSO, CAS 67-68-5), ethylenediaminetetraacetic acid (EDTA, CAS 60-00-4), Tris (CAS 1185-53-1), HEPES (CAS 7365-45-9), ethidium bromide (CAS 1239-45-8), glycerol (CAS 56-81-5), sodium dodecyl sulfate (SDS, CAS 151-21-3), agarose (CAS 9012-36-6), verapamil hydrochloride (CAS 152-11-4), fluorescein (CAS 2321-07-5), $MgCl_2$ (CAS 7786-30-3), KCl (CAS 7447-40-7), boric acid (CAS 10043-35-3), NaOH (CAS 1310-73-2) and NaCl (CAS 7647-14-5), were obtained from Sigma-Aldrich (St. Louis, MO, USA). Dulbecco's modified eagle medium (DMEM), fetal bovine serum (FBS) and Hank's salt solution were purchased from Gibco-Invitrogen (Thermo Fisher Scientific, Waltham, MA, USA) and cisplatin was purchased from Quiral Química do Brasil (Platinil®, Juiz de Fora, Brazil). All the tested complexes were freshly prepared daily.

Synthesis

The ruthenium complexes [Ru(pic)(dppb)(phen)]PF_6 (**SCAR 4**), *cis*-[Ru(pic)$(dppe)_2$]PF_6 (**SCAR 5**) and *cis*-[$RuCl_2$(dppb)(bipy)] (**SCAR 6**) were synthesized at the Federal University of São Carlos, São Carlos, Brazil. The synthesis procedures and characterization tests are described in Queiroz et al. (1998) and Pavan et al. (2010, 2011).

Study of anti-proliferative activity

In vitro cytotoxicity assays on cultured human tumor cell lines still represent the standard method for initial screening of antitumor agents. Thus, as a first step to assess its pharmacological properties, the **SCAR**

complexes were assayed against human colorectal adenocarcinoma Caco-2 [Rio de Janeiro Cell Bank (BCRJ) no. 0059], human prostate carcinoma DU-145 (ATCC® HTB-81™), human cervix adenocarcinoma HeLa (ATCC® CCl-2™), human hepatocellular carcinoma HepG2 (ATCC® HB-8065™), human breast adenocarcinoma MDA-MB-231 (ATCC® HTB-26™) and human normal fibroblasts MRC-5 (ATCC® CCl-171™). All the cells used in this study were obtained from American Type Cell Collection (ATCC) and BCRJ. These tumor and normal cells were cultured in DMEM containing 10% of FBS, at 37 °C in an atmosphere of 5% CO_2 saturation. In vitro anti-proliferative activity for quantitative evaluation was tested by means of the Resazurin (7-hydroxy-3*H*-phenoxazin-3-one-10-oxide sodium) assay. Cells were seeded at a density of 7.5×10^4 cells mL^{-1} in a 96-well plate and incubated for 24 h. On the next day, the tested complexes in stock solutions (1000 μg mL^{-1}) in DMSO were added to the wells. Dilutions of the complexes were prepared to obtain concentrations ranging from 500 to 1.95 μg mL^{-1}. DMSO was used as the vehicle control. Following 24 h of incubation at 37 °C, 50 μL of Resazurin solution (0.01% w/v) was added to each well and the plates were incubated for 2-4 h. The reading was performed in a microplate Synergy H1 (BioTek®) reader using excitation and emission filters at wavelengths of 560 and 590 nm, respectively. The potency of cell growth inhibition for each complex was expressed as an IC_{50} value defined as the concentration that caused 50% inhibition of cell growth.

Topoisomerase IB assays

Purification of human topoisomerase IB

Top 1 was expressed using the galactose inducible promoter in a multi-copy plasmid, YCpGAL1-e-wild type and YCpGAL1-e-Y723F, used for the transformation of EKY3 cells, as described previously (Chillemi et al. 2005). The epitope-tagged constructs contain the N-terminal sequence FLAG: DYKDDDY (indicated with "e"), recognized by the M2 monoclonal antibody. Purification was carried out using an ANTI-FLAG M2 affinity gel (Sigma) column. The FLAG-fusion Top 1 was eluted via competition with five column volumes of a solution containing a 100 μg mL^{-1} FLAG peptide in 50 mM Tris–HCl and 150 mM KCl, pH 7.4. Glycerol was added to each fraction and collected up to a final concentration of 40%. All the fractions were stored at 20 °C. Integrity of the protein was verified by the immunoblot assay. The purified protein was unfolded by SDS-PAGE, transferred to a nitro-cellulose membrane and immunoblotted with a specific monoclonal antibody (Sigma-A9469). An immunoreactive band, corresponding to Top 1, was detected with the BCIP/NBT substrate (Sigma-B3804).

Topoisomerase IB activity in vitro: DNA relaxation assay

The activity of Top 1 was assayed in 30 μL of reaction volume containing 0.5 μg of negatively supercoiled pBlue-Script KSII(+) and reaction buffer (20 mM Tris–HCl, 0.1 mM EDTA, 10 mM $MgCl_2$, 50 μg mL^{-1} acetylated BSA and 150 mM KCl, pH 7.5). The effects of complexes **SCAR** relative to enzyme activity were measured by adding increasing concentrations of the complexes from 0.75 to 400 μM. Reactions were stopped with a final concentration of 0.5% SDS after each time point at 37 °C. The samples were electrophoresed in 1% agarose gel in 50 mM Tris, 45 mM boric acid, and 1 mM EDTA. The gel was stained with ethidium bromide (5 μg mL^{-1}), destained with water and photographed under UV illumination. Wherever indicated, the enzyme and the inhibitor were pre-incubated at 37 °C for 5 min, prior to the addition of the DNA substrate. Assays were performed at least three times, though only one representative gel is shown.

Study of complexes–DNA interactions

Square-wave voltammetry (SWV)

The complexes–DNA interaction studies were performed by SWV. In SWV, a three-electrode system was used, in which glassy carbon was used as a working electrode (GC), Ag/AgCl as a reference electrode and platinum plate as a counter-electrode. The interaction studies were carried out in a Tris–HCl buffer (pH 7.4) 30% DMSO. The titration was performed by adding 50 μL aliquots of ct-DNA (4.2 mM) to an electrochemical cell containing 2 mL of 1.0×10^{-3} M complexes solution.

Viscosity

Viscosity measurements were carried out according to Carter et al. (1989) using an Ostwald viscometer immersed in a water bath maintained at 25 °C. The ct-DNA concentration in the Tris–HCl buffer was kept constant in all samples (4.2 mM), while the concentration of complexes was increased. The flow time was measured at least five times and the mean value was calculated. Data are presented as $(\eta/\eta_0)^{1/3}$ versus the [complex]/[DNA] ratio, where η and η_0 are the specific viscosities of DNA in the presence and absence of the complex, respectively. The values of Z, η and η_0 were calculated using the expression $(t - t_b)/t_b$, where t is the observed flow time and t_b being the flow time of buffer alone (Cohen and Eisenberg 1969; Anbu et al. 2012; Živec et al. 2012).

Study of BSA interactions

Fluorescence spectroscopy is an effective method, which in essence, helps to explore the interactions between small molecules and biomacromolecules. The protein interaction was examined in 96-well plates used for fluorescence assays. BSA (2.5 μM) was prepared by dissolving the protein in buffer (4.5 mM Tris–HCl, 0.5 mM NaOH, and 50 mM NaCl) at pH 7.4. For fluorescence measurements, the BSA concentration in the Tris–HCl buffer was kept constant in all samples, while the concentration of the complexes was increased from 1.56 to 200 μM in DMSO. The quenching of the emission intensity of the BSA's tryptophan residues at 344 nm (excitation wavelength 295 nm) was monitored at varying temperatures (295, 300, 305 and 310 K). Measurements of interaction with BSA were taken using a SpectraMax M3 fluorometer. The experiments were carried out in triplicate and analyzed using the classical Stern–Volmer equation (1):

$$F_0/F = 1 + K_{sv}[Q] = 1 + k_q\tau_0[Q], \quad (1)$$

where F_0 and F are the fluorescence intensities in the absence and presence of quencher, respectively, $[Q]$ being the quencher concentration, and K_{sv} the Stern–Volmer quenching constant, which can be written as $k_q = K_{sv}/\tau_o$, where kq is the bimolecular quenching rate constant and τ_0 being the average lifetime of the fluorophore in the absence of quencher (6.2×10^{-9} s) (Gratton et al. 1992). Therefore, Eq. (1) was applied towards the determination of K_{sv} by linear regression of a plot of F_0/F versus [Q]. The binding constant (K_b) and number of complexes bound to BSA (n) were determined by plotting the double log graph of the fluorescence data using Eq. (2):

$$\log(F_0 - F)/F = \log\ K_b + n \log\ [Q]. \quad (2)$$

The thermodynamic parameters were calculated from the Van't Hoff equation (3):

$$\ln K_b = -(\Delta H^o)/RT + (\Delta S^o)/R, \quad (3)$$

where K is analogous to the Stern–Volmer quenching constant, K_{sv} at the corresponding temperature (the temperatures used were 295, 305 and 310 K), and R being the gas constant, from which the ΔH and ΔS of the reaction can be determined from the linear relationship between $ln\ K$ and the reciprocal absolute temperature. Furthermore, the change in free energy (ΔG) was calculated from the following Eq. (4):

$$\Delta G^o = -RT\ln K = \Delta H^o - T\Delta S^o. \quad (4)$$

The inner filter effect on the intensity of fluorescence of BSA and complexes was previously corrected according to the following Eq. (5) (Lakowicz 1999):

$$F_{corr} = F_{obs}e^{(A_{em}+A_{ex})/2}, \quad (5)$$

where F_{corr} and A_{obs} are the corrected and observed fluorescence intensities, respectively. A_{ex} and A_{em} are the absorbance values of the drugs at the excitation and emission wavelengths, respectively.

Permeation across Caco-2 cells

The Caco-2 assay was conducted in line with Hubatsch et al. (2007). The cells were cultured in 12-well Transwell® (Corning Incorporated, New York, NY) insert filters for 21 days to reach confluence and differentiation at a seeding density of 5×10^4 cells cm^{-2}. The integrity of the monolayer was examined by measuring the transepithelial electrical resistance (TEER) with an epithelial voltammeter Millicell-ERS® (Millipore Corporation, Bedford, MA) and running standard assays using verapamil hydrochloride and fluorescein as paracellular and transcellular flux markers, respectively. Only cell monolayers with a TEER above 300 $\Omega \cdot cm^2$ were used for the transport assays. The complexes were dissolved in DMSO and subsequently diluted in Hank's buffer at pH 7.4 to prepare the permeability samples in

concentrations previously determined by cytotoxic tests. The initial concentrations were 10 μg mL^{-1} for **SCAR 4** and **6**, and 1 μg mL^{-1} for **SCAR 5**. The experiments were initiated with the addition of the complexes solutions in the apical compartment of the Transwell® plates. The basolateral compartment (receptor) was maintained at pH 7.4 with or without the addition of 4.0% (w/v) of BSA. Six replicates of all the complexes were assessed. The plates were kept under stirring at 37 °C in an orbital shaker (25 rpm). The sample collections (200 μL) were taken from the basolateral compartment at 15, 30, 60, 90, 120 and 180 min. After each sampling, the replacement of 200 μL of a fresh permeability buffer with or without BSA, maintained at 37 °C, was preceded in order to maintain the volume in the compartment.

The P_{app} coefficients (cm s^{-1}) were calculated according to the following Eq. (6):

$$P_{app} = VR/(A \times C_0) \times \Delta C/\Delta t, \quad (6)$$

where VR is the volume of the receiver compartment (basolateral), $\Delta C/\Delta t$ being the linear appearance rate of the complexes in the receiver chamber (in ng s^{-1}), A being the membrane surface area (cm^2) while C_0 being the initial concentration in the donor compartment (ng cm^{-3}). For the fact that this calculation requires the fulfilment of the sink conditions, only receiver concentrations below 10% of the donor concentration were employed in the calculations.

UPLC analysis

The samples were quantified by means of ultra-high performance liquid chromatography with UV (UHPLC-UV) detection in a Waters Acquity® UPLC H-Class coupled to a computer system for data acquisition (Empower®, Waters). The method was validated according to Baka et al. (2008). Chromatographic separations were obtained using an Acquity UPLC CSH C18 column (1.7 μm 2.1 × 50 mm) at 40 °C. The mobile phase (0.4 mL min^{-1}) was composed of acetonitrile and 1% formic acid in water (65:35). The analytical wavelength was set at 370 nm and samples of 1 μL were injected into the UPLC system.

Lipophilicity measurements

The octanol–water partition coefficient (log P) were determined using the stir-flask method (Baka et al. 2008). Each complex was tested in a mixture of equal volumes of water and octanol with continuous shaking for 24 h at 1000 rpm and 37 °C. Then the samples were centrifuged for 5 min at 300 rpm and the organic and aqueous phases were separated. The concentration of drug in each phase was measured spectrophotometrically in order to determine values of log P = [drug] (in *n*-octanol)/[drug] (in water). The experiments were carried out in triplicate.

Results and discussion

Anti-proliferative activity

The anti-proliferative activities of the three complexes were assessed using Resazurin assay, monitoring their capacities to inhibit Caco-2, DU-145, HeLa, HepG2 and MDA-MB-231 cell growth. Cisplatin (Platinil®) was the reference cytotoxic drug. The results were expressed by determining the IC_{50} values which have been summarized in Table 1.

The selectivity index (SI) of each complex was determined as the ratio of IC_{50} of MRC-5 normal cells to IC_{50} of tumor cells.

The complexes displayed cytotoxicity against cancer cells, furthermore both prostate and breast tumor cells shows the highest sensitivity to the all three complexes compared to other tumor cells. It is worth noting that the ruthenium(II) complexes were found to be relatively more active compared to cisplatin. A comparison between the complexes revealed that **SCAR 5** is potent against all cancer cell lines, while **SCAR 4** is more cytotoxic against prostate and breast cells. **SCAR 6** was found to be less cytotoxic though it bears the highest SI.

SCAR 5 has a bidentate phosphine, which could explain the increased cytotoxicity, compared to **SCAR 4**. The addition of phosphine is seen to increase the lipophilicity of the complex, which in turn enhances the cytotoxic activity (Motswainyana and Ajibade 2015). Other studies show that the addition of phosphine ligands in gold(I) complexes gives rise to a significant increase in the cytotoxic effect in relation to metal free (McKeage et al. 2000). The use of pyridyl phosphine bidentate ligands was found to increase the lipophilicity and hepatotoxicity of some complexes in vitro, while considerably affecting the uptake by tumor cells and proteins binding (McKeage et al. 2000; Liu et al. 2008).

Table 1 Cytotoxicity activity of complexes **SCAR** and cisplatin on colon (Caco-2), prostate (DU-145), cervix (HeLa), liver (HepG2) and breast (MDA-MB-231) cancer cells and on normal fibroblasts (MRC-5)

Cells	**SCAR 4**		**SCAR 5**		**SCAR 6**		Cisplatin	
	$IC_{50} \pm SD$	SI[c]	$IC_{50} \pm SD$	SI[c]	$IC_{50} \pm SD$	SI[c]	$IC_{50} \pm SD$	SI[c]
MRC-5[a]	47.4 ± 1.7	–	6.8 ± 0	–	551.7 ± 19.2	–	13.0 ± 1.1	–
Caco-2[b]	14.8 ± 2.1	3.2	4.2 ± 0.9	1.6	130.4 ± 9.2	4.2	19.0 ± 5.2	0.7
DU-145[b]	5.7 ± 1.5	8.3	1.5 ± 0.5	4.5	43.4 ± 4.7	12.7	46.0 ± 3.5	0.3
HeLa[b]	44.9 ± 7.4	1.0	8.7 ± 1.5	0.8	252.6 ± 12.2	2.2	21.0 ± 2.1	0.6
HepG2[b]	60.9 ± 6.7	0.8	3.5 ± 1.1	1.9	137.3 ± 11.7	4.0	14.1 ± 3	0.9
MDA-MB-231[b]	4.0 ± 0.9	11.8	1.5 ± 0.5	4.5	42.3 ± 8.9	13.0	69.2 ± 4.2	0.2

IC_{50} values were determined from three independent experiments using concentration (μM) in triplicate

IC_{50} inhibitory concentration to 50%, *SI* selectivity index

[a] Determined in normal cells after 24 h incubation with complexes and cisplatin

[b] Determined in cancer cells after 24 h incubation with complexes and cisplatin

[c] SI determined as (IC_{50} normal cells)/(IC_{50} tumor cells)

Opposed to **SCAR 4** and **5**, the **SCAR 6** showed high values for IC_{50}. However, **SCAR 6** showed higher selectivity for breast cells (SI >10), whereas cisplatin showed a high IC_{50} for the same cells and devoid of selectivity (Table 1).

Topoisomerase IB activity

The role of complexes **SCAR** in the inhibition of the relaxation activity of Top 1 was assessed by a plasmid relaxation assay, incubating a supercoiled plasmid with the enzyme in the absence or presence of different complexes concentrations (Fig. 2). The relaxation activity monitored at 10 min following incubation indicates that the complexes inhibit Top 1 activity in a dose dependent manner, and **SCAR 5** is found to be the most active complex in that a full Top 1 inhibition is achieved at 12.5 μM (Fig. 2(B), lane 8), while the same is only found to occur at 200 μM for **SCAR 4** (Fig. 2(A), lane 12). For **SCAR 6**, a full inhibition was not achieved, even at a very high concentration of the complex, the reason possibly related to the interaction with the DNA substrate. The band of the supercoiled plasmid, in the absence of an enzyme, has an identical height in the absence and presence of a large complex concentration indicating that **SCAR 4** and **5** do not, in effect, interact with the DNA substrate at this concentration (Fig. 2(A,B) lane 13). We suggest that the higher molecular volume of **SCAR 5**, presenting two phosphine ligands, is likely to contribute towards the inhibition capacity of **SCAR 5** compared to **SCAR 4**, by directly binding to Top 1 or Top 1–DNA complex.

A lower concentration of **SCAR 5** is found to be sufficient to cause a complete inhibition of Top 1

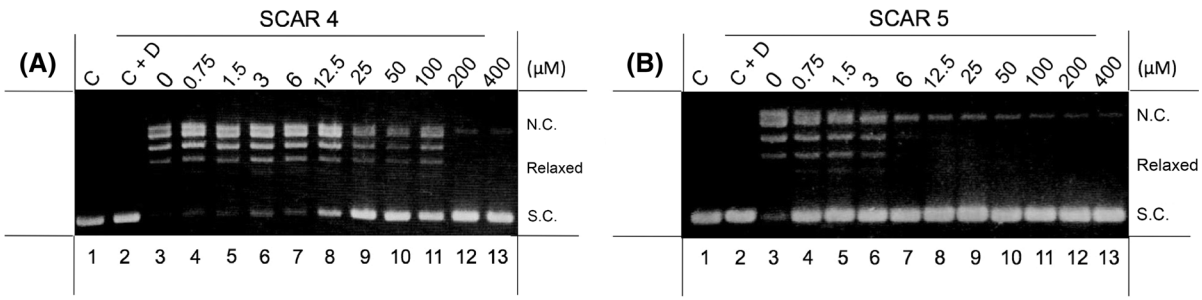

Fig. 2 Relaxation of negative supercoiled plasmid DNA by topoisomerase IB in the presence of increasing concentrations of **SCAR 4** (**a**) and **SCAR 5** (**b**). The reaction products were resolved in an agarose gel and visualized with ethidium bromide. *Lane 1* DNA substrate. *Lane 2* DNA plus DMSO. *Lane 3* DNA plus enzyme, *NC* nicked circular plasmid DNA, *SC* supercoiled plasmid DNA

activity, when the complex is pre-incubated with the enzyme. In detail, a concentration of 1.25 μM of **SCAR 5** fully inhibits the enzyme when pre-incubated for 5 min prior to the addition of the DNA substrate, implying that the complex directly interacts with the enzyme (Fig. 3, lanes 14–19).

Low IC_{50} values and potent Top 1 inhibition show that **SCAR 5** is a promising candidate for anticancer therapy. The high cytotoxicity in tumor cells, mainly derived from prostate and breast carcinomas can be explained by a largely high activity of Top 1 inhibition, causing the blockage of Top 1 cleavage complex or the inhibition of catalytic activity of Top 1 (Barros et al. 2013). The inhibition of Top 1 undermines the enzyme's capacity to regulate the number of topological connections of the DNA strands (Roca 1995). The inhibition of this activity causes DNA damage and thus leading to cell death (Hong and Kreuzer 2000; He et al. 2014).

Considering that tumor cells often show increased amounts of Top 1, these cells should be more sensitive to the effects of enzyme inhibitors (Barros et al. 2013). This fact may support the cytotoxic and selective effects of **SCAR 4** and **5**. Nevertheless, the exact mechanism of this activity needs to be given a more detailed assessment.

Complexes–DNA interactions

Square-wave voltammetry (SWV)

The investigation of the interaction of complexes **SCAR** with DNA through SWV indicates a shift of the redox potential toward negative values, with Δ of 39 mV for **SCAR 4** and 19 mV for **SCAR 5** (Fig. 4), which is an indicative of an electrostatic complexes–DNA interaction, probably through the phosphate group of the DNA backbone which is negatively

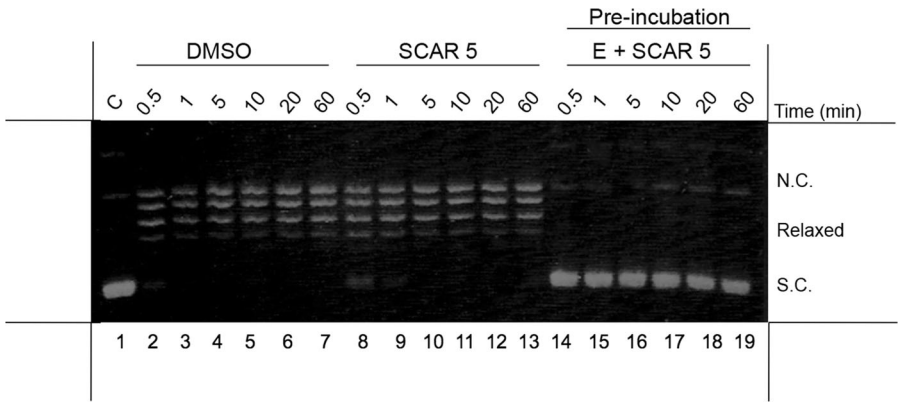

Fig. 3 Relaxation of negative supercoiled plasmid DNA in a time course experiment with DMSO (*lanes 2–7*), in the presence of 1.25 μM **SCAR 5** (*lanes 8–13*), after pre-incubation enzyme and 1.25 μM **SCAR 5** for 5 min at 37 °C (*lanes 14–19*). *Lane 1* no protein added

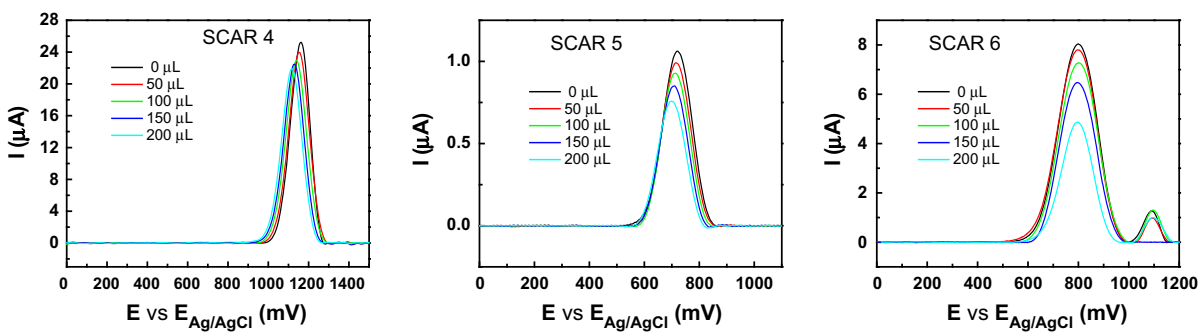

Fig. 4 Square-wave voltammograms of **SCAR 4–6** (1.0 mM) at the GC electrode in Tris–HCl buffer (pH 7.4), 30% DMSO was used as a supporting electrolyte, DNA 4.2 mM. Frequency 50 Hz, pulse height 75 mV and potential increment 2 mV

charged, while the complexes have a positive charge (Da Silva et al. 2012; Sirajuddin et al. 2013). Interestingly, no displacement was observed for **SCAR 6** ($\Delta = 0$), due to ct-DNA precipitation during the titration. Therefore, aiming at clarifying the type of interaction between the complex and the ct-DNA, viscosity measurements were made in the presence and absence of the complexes.

Viscosity

The effect of the complexes vis-à-vis the perturbation of the DNA viscosity is depicted in Fig. 5. No significant change is observed by changing the concentration of the **SCAR 4** and **5**, indicating that these complexes do not intercalate to the DNA and that the complexes–DNA interaction has mainly an electrostatic character (Queiroz et al. 1998) as also suggested by the SWV measurements.

SCAR 6, however, led to a decrease of the DNA viscosity by increasing concentration of the complex on ct-DNA. These findings indicate that **SCAR 6** interacts by non-classical or covalent interleaving which results in a local curving or twisting of the DNA helix, reducing their effective length and there by engendering the decrease in viscosity of the DNA solution (Kelly et al. 1885; Liu et al. 2002). This result has a typical profile of cisplatin (Fig. 5), known to cause a 'shortening effect' in the DNA due to the covalent bond which determines the decrease in viscosity (Selvi and Palaniandavar 2002; Kathiresan et al. 2015). The covalent interaction suggested for the **SCAR 6** can be explained by the possible hydrolysis of its chloride ligands. The generation of somewhat seemingly "bis-aqua" species has the likelihood of binding irreversibly to the DNA, a square planar structure of cisplatin for instance (Kelland 2007; Page 2012). This interaction may cause DNA breaks, and consequently, micronuclei formation as evidenced (De Grandis et al. 2016) in HepG2 cells. The failure or perhaps the inability to explain the results of the DNA relaxation assay can also be attributed to the interaction. Probably, **SCAR 6** may well interact with the DNA substrate though the enzyme activity could not be evaluated.

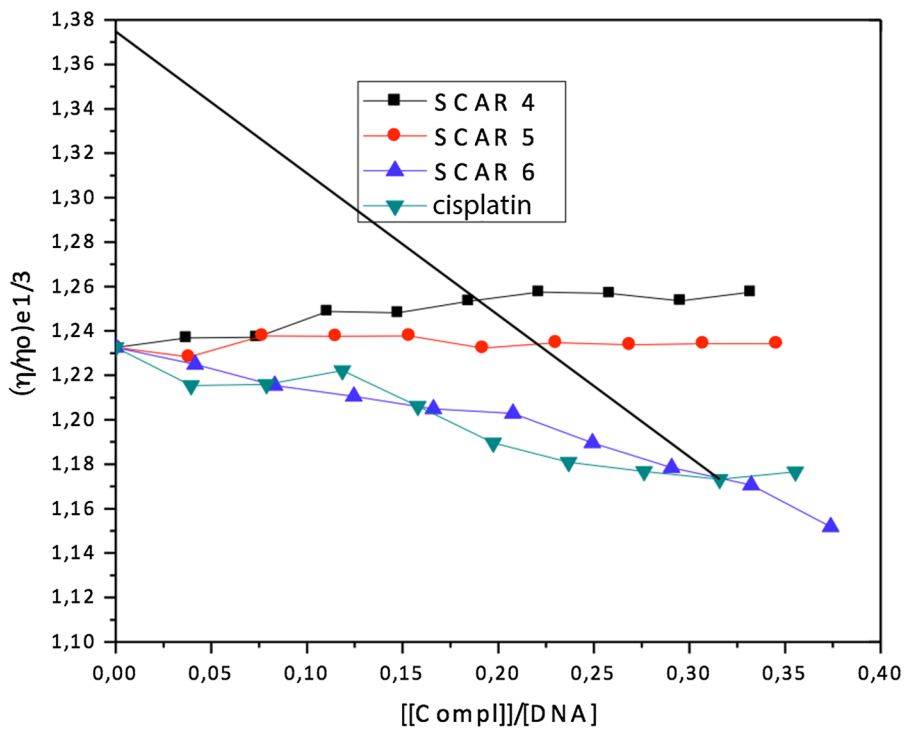

Fig. 5 Effect of concentration of complexes **SCAR** related to the viscosity of DNA (4.2 mM), at 298 K

Complexes–BSA interactions

The fluorescence quenching has been studied at varying temperatures so as to discriminate between static and dynamic quenching (Lakowicz 1999). Higher temperatures result in faster diffusion and hence a larger degree of collisional quenching. They may also propel the dissociation of weakly bound complexes, thus leading to less static quenching. As shown in Fig. 6, BSA showed strong fluorescence emission, while the complexes displayed almost no intrinsic fluorescence under the experimental conditions used for the measurements. The fluorescence intensity of BSA was found to diminish relative to an increase in the complexes concentrations, accompanied by a red shift in the maximum emission wavelengths in the fluorescence spectra. In order to ascertain the fluorescence quenching mechanism, the fluorescence quenching data were measured at different temperatures (295, 300, 305 and 310 K).

These results show that in **SCAR 4** and **5**, the K_{sv} values decreases when the temperature is increased (Table 2), with the exception of **SCAR 6**. Moreover, the values of k_q for all complexes were in the range of 2.42×10^{12}–38.51×10^{12} mol L^{-1}, far higher than 2.0×10^{10} mol L^{-1}, the maximum possible value for dynamic quenching, indicating the existence of static quenching mechanism. The quenching data for the static quenching process were analyzed according to the modified Stern–Volmer equation equation (2). The binding constants K_b and binding sites, n, were calculated from the slopes of the static quenching equation: $\log(F_0 - F)/F$ versus log[Q].

The results are summarized in Table 2. The K_b for **SCAR 4** and **5**, with BSA ranging between 10^3 and 10^4 M^{-1}, the results pointing out that the complexes tend to bind to a single specific site, given the n value approximation to 1. The interaction between **SCAR 6** and BSA presents much higher K_b values, indicating that the presence of chloride ligands in place of picolinate increases the binding affinity with BSA in the order of 10^6 M^{-1}.

Although the interaction between the complex and the BSA is essentially desirable, this interaction should be, in effect, reversible. It should be low enough to enable us attain the expected goal regarding the complex to be released, which may fail to occur once the interaction happens to be very strong, so that the complex remains bound to albumin indefinitely (Hu et al. 2005; Elsadek and Kratz 2012). The interaction between the complexes and BSA is found to be are predominantly hydrophobic character, characterized by an intermediate ΔG value since both the enthalpic and entropic terms are positive and it is likely that it occurs in the proximity of Trp-212. The magnitude of the BSA-binding constant of **SCAR 4** and **5**, compared with other ruthenium(II) complexes reported recently (Colina-Vegas et al. 2015; Camargo et al. 2016) suggests a relatively moderate interaction with the BSA molecule, while **SCAR 6** shows a stronger interaction with the protein.

In vitro permeability of complexes

Over the last years, Caco-2 cell membranes have been widely employed for the screening of intestinal permeation of new compounds owing to the fact that the transport of drugs across the Caco-2 cell monolayers is correlated with the bioavailability and oral absorption in vivo (Artursson and Karlsson 1991;

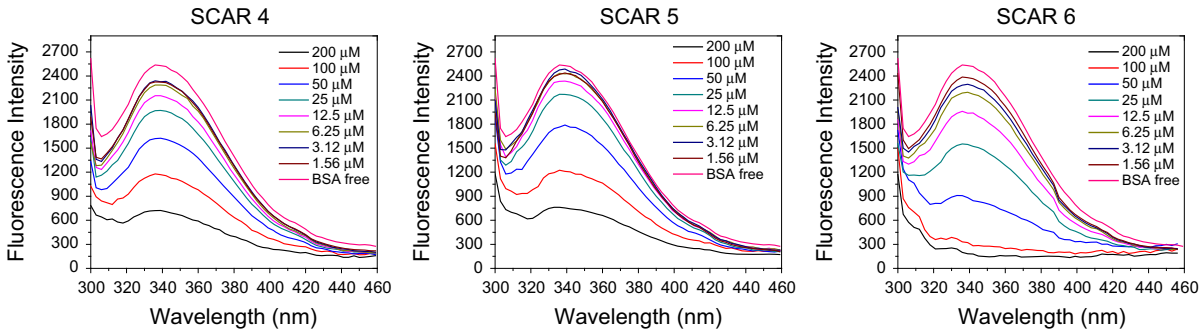

Fig. 6 Fluorescence quenching spectra of BSA at different concentrations of complexes **SCAR** at 37 °C temperature, excitation wavelength 295 nm

Table 2 BSA–**SCAR** interactions and thermodynamic parameters

Complexes	T (K)	K_{sv} (10^4 L mol^{-1})	k_q (10^{12} L mol^{-1} s^{-1})	K_b	n	ΔH° (kJ mol^{-1} K^{-1})	ΔS° (J mol^{-1} K^{-1})	ΔG° (kJ mol^{-1})
SCAR 4	295	1.594 ± 0.076	2.571	(1.345 ± 0.691) × 10^3	0.735	8.249	88.278	−17.792
	300	1.595 ± 0.059	2.573	(1.595 ± 0.862) × 10^3	0.751			−18.234
	305	1.581 ± 0.065	2.550	(1.592 ± 0.851) × 10^3	0.754			−18.676
	310	1.581 ± 0.069	2.550	(1.621 ± 0.929) × 10^3	0.757			−19.117
SCAR 5	295	1.516 ± 0.077	2.445	(1.501 ± 0.256) × 10^4	1.031	53.019	261.617	−24.158
	300	1.515 ± 0.073	2.444	(3.829 ± 0.556) × 10^4	1.162			−25.466
	305	1.502 ± 0.055	2.422	(3.946 ± 0.918) × 10^4	1.162			−26.774
	310	1.502 ± 0.050	2.422	(4.711 ± 1.512) × 10^4	1.178			−28.082
SCAR 6	295	22.607 ± 1.759	36.462	(1.912 ± 0.309) × 10^6	1.178	31.607	227.280	−35.440
	300	22.923 ± 2.014	36.973	(3.033 ± 0.554) × 10^6	1.308			−36.577
	305	23.097 ± 1.789	37.253	(2.998 ± 0.430) × 10^6	1.361			−37.713
	310	23.880 ± 1.157	38.516	(3.828 ± 0.289) × 10^6	1.362			−38.849

Lipinski et al. 2001; Hubatsch et al. 2007; Hernández et al. 2010). The use of TEER parameter as an indicator of integrity of the Caco-2 membrane has been largely applied in this technique, while significant correlations between the TEER values and permeability of complexes absorbed by the paracellular route have been obtained. A further way of assessing membrane integrity and viability during the permeability experiments is by determining the permeability of complexes with the well-known P_{app} data. Fluorescein and verapamil were used in this study as low and high permeability standards, respectively, to assess the adequacy and integrity of the culture conditions of the Caco-2 cell membranes. The mean of the P_{app} values obtained for fluorescein and verapamil was 0.11×10^{-6} and 41.08×10^{-6} cm s^{-1}, respectively. These values are in agreement with those obtained in the literature, indicating the adequacy of the cultivation conditions of Caco-2 cells as well as the reliability of the results obtained for the complexes (Gonçalves et al. 2012; Chang et al. 2013).

According to the classification proposed by Yee (1997), in tests without the addition of 4.0% (w/v) BSA, **SCAR 4–6** can be classified as moderately, well and poorly absorbed drugs, respectively. The high lipophilicity of **SCAR 5** may have contributed in increasing the P_{app} value, promoting its permeation through the Caco-2 cell membrane (Table 3). The higher lipophilicity likewise the consequent permeability can be attributed to the presence of additional phosphine ligand to the molecule. As demonstrated, the use of diphosphines as ligands can adjust the lipophilic/hydrophilic balance in gold complexes, where in general, its activity is found to increase thanks to an increase in the lipophilicity (Lima and

Table 3 Log P and P_{app} values of complexes **SCAR** determined from the amount permeated through the Caco-2 cells monolayers in presence and absence of BSA 4% (w/v) in receptor chamber

Complexes	log P	P_{app} (10^{-6} cm s^{-1})[a]	
		(−)BSA	(+)BSA
SCAR 4	0.14 ± 0.05	9.07 ± 1.60	11.13 ± 2.80
SCAR 5	0.35 ± 0.01	15.34 ± 1.81	24.71 ± 3.92*
SCAR 6	−0.40 ± 0.03	0.38 ± 0.07	5.07 ± 0.02*

* All p values are <0.05

[a] Mean ± SD ($n = 6$)

Rodríguez 2011). Studies conducted on Caco-2 monolayers showed that the permeability of different drugs increases with the increase in their lipophilicity, where one can cite, for instance, the accumulation observed in the jejunal mucosa of rats for the most lipophilic drugs (Yamashita et al. 1997).

SCAR 6 is found to exhibit low permeation through the membrane of Caco-2. Indeed, the relationship between log P and oral absorption undoubtedly merits the consideration of the charge of ionizable groups of compounds that plays a key role as far as the membrane permeation rate is concerned (Veber et al. 2002; Doak et al. 2014). According to the five rules proposed by Lipinski et al. (1997, 2001), approximately 90% of the drugs, among other parameters, have their passive absorption via cell membranes associated with lipophilicity when log P is in the range ≤ 5 and ≥ 0. Accordingly, the log P of -0.40 presented by **SCAR 6** may hinder its permeation on Caco-2 monolayers, thus explaining its low P_{app} values (Table 3).

The effect of BSA on the permeation of the complexes was evaluated through the addition of BSA in the basolateral compartment. This strategy is found to be essentially useful when it comes to the determination of lipophilic drugs permeability which tend to accumulate within cells or even adsorb to the plastic filters (Fossati et al. 2008; Krishna et al. 2001). In these tests, **SCAR 5** and **6** were found to present a significant increase ($p < 0.05$) in the P_{app} (24.71×10^{-6} and 5.07×10^{-6} cm s^{-1}, respectively; Table 3). With regard to low lipophilic complexes as **SCAR 6**, the BSA in the receptor compartment is expected to aid the P_{app}, considering that the presence of the protein in the buffer contributes towards preventing the return in the opposite direction of the absorption (Krishna et al. 2001).

Conclusion

Several biological properties of ruthenium(II) phosphine/diimine/picolinate complexes have been here in demonstrated. Our findings show the antiproliferative activity of complexes **SCAR 4** and **5** against the Caco-2, DU-145, HeLa, HepG2 and MDA-MB-231 cell lines to be 45 times higher compared to the metallodrug cisplatin (Table 1). One possible target of this class of complexes has to do with human topoisomerase I, given that **SCAR 4** and **5** inhibit the DNA relaxation of Top 1 in a dose dependent manner (Fig. 2). **SCAR 5** is found to be the most efficient complex which when pre-incubated with the enzyme displays an enhanced inhibitory capacity, suggesting that it directly interacts with the Top 1 (Fig. 3). Thus, **SCAR 5** can be said to act both as a Top 1 inhibitor and a cytotoxic agent, meriting further advanced investigation for it to be better explored as a possible anticancer drug. The complexes/DNA interaction studies carried out show that **SCAR 4** and **5** can bind to DNA through electrostatic interactions while **SCAR 6** via covalent interactions. The complexes/BSA binding studies indicate a spontaneous interaction between these two species besides the presence of hydrophobic forces between them. **SCAR 4** and **5** can both be considered as high oral absorption candidates with potential application via enteral, being largely more convenient, safe and economical. **SCAR 6**, despite presenting low in vitro permeation, may still have the oral absorption problems improved with the use of pharmacothecnical tools, such as the incorporation of nanoparticles. This work points out that these complexes are suitable compounds for drug development and the studies presented here pave the way for the elucidation of their mechanisms of action as possible antitumor drugs.

Acknowledgements The authors would like to express their deepest gratitude and indebtedness to the São Paulo Research Foundation (FAPESP Grants 2012/22364-1 and 2013/20078-4) and Coordinating Committee for Advancement of Higher Education Staff in Brazil (CAPES) for the financial support granted during the course of this work. Our thanks also go to Michel L. de Campos for his support with the UPLC analysis.

Compliance with ethical standards

Conflict of interest The authors declare that they have no conflicts of interest regarding the contents of this article.

References

Allardyce CS, Dyson PJ (2001) Ruthenium in medicine: current clinical uses and future prospects. Platin Met Rev 45:62–69

Allardyce CS, Dyson PJ (2016) Metal-based drugs that break the rules. Dalton Trans 45:3201–3209. doi:10.1039/C5DT03919C

Anbu S, Ravishankaran R, Karande AA, Kandaswamy M (2012) DNA targeting polyaza macrobicyclic dizinc(II) complexes promoting high *in vitro* caspase dependent antiproliferative activity against human carcinoma cancer cells. Dalton Trans 41:12970. doi:10.1039/c2dt31094e

Artursson P, Karlsson J (1991) Correlation between oral drug absorption in humans and apparent drug permeability coefficients in human intestinal epithelial (Caco-2) cells. Biochem Biophys Res Commun 175:880–885. doi:10.1016/0006-291X(91)91647-U

Artursson P, Palm K, Luthmanb K (2001) Caco-2 monolayers in experimental and theoretical drug transport predictions of drug transport. Adv Drug Deliv Rev 46:27–43

Baka E, Comer JEA, Takács-Novák K (2008) Study of equilibrium solubility measurement by saturation shake-flask method using hydrochlorothiazide as model compound. J Pharm Biomed Anal 46:335–341. doi:10.1016/j.jpba.2007.10.030

Barros FWA, Bezerra DP, Ferreira PMP et al (2013) Inhibition of DNA topoisomerase I activity and induction of apoptosis by thiazacridine derivatives. Toxicol Appl Pharmacol 268:37–46. doi:10.1016/j.taap.2013.01.010

Barton JK, Olmon ED, Sontz PA (2011) Metal complexes for DNA-mediated charge transport. Coord Chem Rev 255:619–634

Camargo MS, da Silva MM, Correa RS et al (2016) Inhibition of human DNA topoisomerase IB by nonmutagenic ruthenium(II)-based compounds with antitumoral activity. Metallomics 8:179–192. doi:10.1039/c5mt00227c

Carter MT, Rodriguez M, Bard AJ (1989) Voltammetric studies of the interaction of metal chelates with DNA. 2. Tris-chelated complexes of cobalt(III) and iron(II) with 1,10-phenanthroline and 2,2-bipyridine. J Am Chem Soc 111:8901–8911. doi:10.1021/ja00206a020

Chang M, Li X, Sun Y et al (2013) A potential mechanism of a cationic cyclopeptide for enhancing insulin delivery across Caco-2 cell monolayers. Biol Pharm Bull 36:1602–1607. doi:10.1248/bpb.b13-00487

Chillemi G, Fiorani P, Castelli S et al (2005) Effect on DNA relaxation of the single *Thr718Ala* mutation in human topoisomerase I: a functional and molecular dynamics study. Nucleic Acids Res 33:3339–3350. doi:10.1093/nar/gki642

Cohen G, Eisenberg H (1969) Viscosity and sedimentation study of sonicated DNA-proflavine complexes. Biopolymers 8:45–55. doi:10.1002/bip.1969.360080105

Colina-Vegas L, Villarreal W, Navarro M et al (2015) Cytotoxicity of Ru(II) piano-stool complexes with chloroquine and chelating ligands against breast and lung tumor cells: interactions with DNA and BSA. J Inorg Biochem 153:150–161. doi:10.1016/j.jinorgbio.2015.07.016

Corrêa RS, da Silva MM, Graminha AE et al (2016) Ruthenium(II) complexes of 1,3-thiazolidine-2-thione: cytotoxicity against tumor cells and anti-*Trypanosoma cruzi* activity enhanced upon combination with benznidazole. J Inorg Biochem 156:153–163. doi:10.1016/j.jinorgbio.2015.12.024

Da Silva LL, Donnici CL, Lopes JCD et al (2012) Investigação eletroquímica e calorimétrica da interação de novos agentes antitumorais biscatiônicos com DNA. Quim Nova 35:1318–1324

De Grandis RA, Resende FA, Da Silva MM et al (2016) *In vitro* evaluation of cyto-genotoxic potential of ruthenium(II) SCAR complexes: a promising class of antituberculosis agents. Mutat Res Genet Toxicol Environ Mutagen 798–799:11–18. doi:10.1016/j.mrgentox.2016.01.007

Doak BC, Over B, Giordanetto F, Kihlberg J (2014) Oral druggable space beyond the rule of 5: insights from drugs and clinical candidates. Chem Biol 21:1115–1142. doi:10.1016/j.chembiol.2014.08.013

Elsadek B, Kratz F (2012) Impact of albumin on drug delivery—new applications on the horizon. J Control Release 157:4–28. doi:10.1016/j.jconrel.2011.09.069

Fossati L, Dechaume R, Hardillier E et al (2008) Use of simulated intestinal fluid for Caco-2 permeability assay of lipophilic drugs. Int J Pharm 360:148–155. doi:10.1016/j.ijpharm.2008.04.034

Gonçalves JE, Ballerini Fernandes M, Chiann C et al (2012) Effect of pH, mucin and bovine serum on rifampicin permeability through Caco-2 cells. Biopharm Drug Dispos 33:316–323

Gou Y, Zhang Y, Qi J et al (2015) Enhancing the copper(II) complexes cytotoxicity to cancer cells through bound to human serum albumin. J Inorg Biochem 144:47–55. doi:10.1016/j.jinorgbio.2014.12.012

Gratton E, Silva N, Mei G et al (1992) Fluorescence lifetime distribution of folded and unfolded proteins. Int J Quantum Chem 42:1479–1489. doi:10.1002/qua.560420522

Grès M, Julian J, Bourriè M et al (1998) Correlation between oral drug absorption in humans, and apparent drug permeability in TC-7 cells, a human epithelial intestinal cell line: comparison with the parental Caco-2 cell line. Pharm Res 15:726–733

He X, Jin L, Tan L (2014) DNA-binding, topoisomerases I and II inhibition and *in vitro* cytotoxicity of ruthenium(II) polypyridyl complexes: $[Ru(dppz)_2L](^{2+})$ (L = dppz-11-CO_2-Me and dppz). Spectrochim Acta A 135C:101–109. doi:10.1016/j.saa.2014.06.147

Hernández R, Méndez J, Lamboy J et al (2010) Titanium(IV) complexes: cytotoxicity and cellular uptake of titanium(IV) complexes on caco-2 cell line. Toxicol In Vitro 24:178–183. doi:10.1016/j.tiv.2009.09.010

Hong G, Kreuzer KN (2000) An antitumor drug-induced topoisomerase cleavage complex blocks a bacteriophage T4 replication fork *in vivo*. Mol Cell Biol 20:594–603. doi:10.1128/MCB.20.2.594-603.2000.Updated

Hu YJ, Liu Y, Zhao RM, Qu SS (2005) Interaction of colchicine with human serum albumin investigated by spectroscopic methods. Int J Biol Macromol 37:122–126. doi:10.1016/j.ijbiomac.2005.09.007

Hubatsch I, Ragnarsson EGE, Artursson P (2007) Determination of drug permeability and prediction of drug absorption in Caco-2 monolayers. Nat Protoc 2:2111–2119. doi:10.1038/nprot.2007.303

Kathiresan S, Dhivya R, Vigneshwar M et al (2015) Biological evaluation of redox stable cisplatin/Cu(II)–DNA adducts as potential anticancer agents. J Coord Chem 8972:1–15. doi:10.1080/00958972.2015.1105366

Kelland L (2007) The resurgence of platinum-based cancer chemotherapy. Nat Rev Cancer 7:573–584. doi:10.1038/nrc2167

Kelly JM, Tossi AB, MacConnell DJ, OhUigin C (1885) A study of the interactions of some polypyridylruthenium(II) complexes with DNA using fluorescence spectroscopy,

topoisomerisation and thermal denaturation. Nucleic Acids Res 13:6017–6034. doi:10.1093/nar/gkq840

Krishna G, Chen KJ, Lin CC, Nomeir AA (2001) Permeability of lipophilic compounds in drug discovery using *in vitro* human absorption model, Caco-2. Int J Pharm 222:77–89. doi:10.1016/S0378-5173(01)00698-6

Lakowicz JR (1999) Principles of fluorescence spectroscopy. Kluwer Academic/Plenum Publishers, New York, pp 1–24

Li L-Y, Jia H-N, Yu H-J et al (2012) Synthesis, characterization, and DNA-binding studies of ruthenium complexes $[Ru(tpy)(ptn)]^{2+}$ and $Ru(dmtpy)(ptn)]^{2+}$. J Inorg Biochem 113:31–39. doi:10.1016/j.jinorgbio.2012.03.008

Lima CJ, Rodríguez L (2011) Phosphine–gold(I) compounds as anticancer agents: general description and mechanisms of action. Anticancer Agents Med Chem 11:921–928

Lipinski CA, Lombardo F, Dominy BW, Feeney PJ (1997) Experimental and computational approaches to estimate solubility and permeability in drug discovery and developmental settings. Adv Drug Deliv Rev 23:3–25. doi:10.1016/S0169-409X(96)00423-1

Lipinski CA, Lombardo F, Dominy BW, Feeney PJ (2001) Experimental and computational approaches to estimate solubility and permeability in drug discovery and development settings. Adv Drug Deliv Rev 64:4–17. doi:10.1016/j.addr.2012.09.019

Liu J, Zhang T, Lu T et al (2002) DNA-binding and cleavage studies of macrocyclic copper(II) complexes. J Inorg Biochem 91:269–276

Liu JJ, Galettis P, Farr A et al (2008) *In vitro* antitumour and hepatotoxicity profiles of Au(I) and Ag(I) bidentate pyridyl phosphine complexes and relationships to cellular uptake. J Inorg Biochem 102:303–310. doi:10.1016/j.jinorgbio.2007.09.003

Lu Y, Mahato RI (2009) Pharmaceutical perspectives of cancer therapeutics. Springer, Dordrecht

McKeage MJ, Berners-Price SJ, Galettis P et al (2000) Role of lipophilicity in determining cellular uptake and antitumour activity of gold phosphine complexes. Cancer Chemother Pharmacol 46:343–350. doi:10.1007/s002800000166

Messori L, Camarri M, Ferraro T et al (2013) Promising *in vitro* anti-Alzheimer properties for a ruthenium(III) complex. ACS Med Chem Lett 4:329–332. doi:10.1021/ml3003567

Motswainyana WM, Ajibade PA (2015) Anticancer activities of mononuclear ruthenium(II) coordination complexes. Adv Chem 2015:1–21. doi:10.1155/2015/859730

Nišavić M, Masnikosa R, Butorac A et al (2016) Elucidation of the binding sites of two novel Ru(II) complexes on bovine serum albumin. J Inorg Biochem 159:89–95. doi:10.1016/j.jinorgbio.2016.02.034

Page S (2012) Ruthenium compounds as anticancer agents. Education in Chemistry. http://www.rsc.org/images/Anticancer%20Drugs_EiC_January2012_tcm18-212416.pdf. Accessed 27 Sept 2016

Pavan FR, Von Poelhsitz G, do Nascimento FB et al (2010) Ruthenium(II) phosphine/picolinate complexes as antimycobacterial agents. Eur J Med Chem 45:598–601. doi:10.1016/j.ejmech.2009.10.049

Pavan FR, Poelhsitz GV, Barbosa MIF et al (2011) Ruthenium(II) phosphine/diimine/picolinate complexes: inorganic compounds as agents against tuberculosis. Eur J Med Chem 46:5099–5107. doi:10.1016/j.ejmech.2011.08.023

Pavan FR, Poelhsitz GV, da Cunha LVP et al (2013) *In vitro* and *in vivo* activities of ruthenium(II) phosphine/diimine/picolinate complexes (SCAR) against *Mycobacterium tuberculosis*. PLoS ONE 8:1–10. doi:10.1371/journal.pone.0064242

Queiroz SL, Batista AA, Oliva G et al (1998) The reactivity of five-coordinate Ru(II) (1,4-*bis*(diphenylphosphino)butane) complexes with the *N*-donor ligands: ammonia, pyridine, 4-substituted pyridines, 2,2′-bipyridine, *bis*(*o*-pyridyl)amine, 1,10-phenanthroline, 4,7-diphenylphenanthroline and ethylened. Inorg Chim Acta 267:209–221. doi:10.1016/S0020-1693(97)05615-6

Roca J (1995) The mechanisms of DNA topoisomerases. Trends Biochem Sci 20:156–160. doi:10.1016/S0968-0004(00)88993-8

Selvi PT, Palaniandavar M (2002) Spectral, viscometric and electrochemical studies on mixed ligand cobalt(III) complexes of certain diimine ligands bound to calf thymus DNA. Inorg Chim Acta 337:420–428. doi:10.1016/S0020-1693(02)01112-X

Sirajuddin M, Ali S, Badshah A (2013) Drug–DNA interactions and their study by UV–visible, fluorescence spectroscopies and cyclic voltammetry. J Photochem Photobiol B 124:1–19. doi:10.1016/j.jphotobiol.2013.03.013

Stenberg P, Norinder U, Luthman K, Artursson P (2001) Experimental and computational screening models for the prediction of intestinal drug absorption. J Med Chem 44:1927–1937. doi:10.1021/jm001101a

Veber DF, Johnson SR, Cheng H et al (2002) Molecular properties that influence the oral bioavailability of drug candidates. J Med Chem 45:2615–2623. doi:10.1021/jm020017n

Yamashita S, Tanaka Y, Endoh Y et al (1997) Analysis of drug permeation across Caco-2 monolayers—implications for predicting *in vivo* drug absorption. Pharm Res 14:486–491

Yee S (1997) *In vitro* permeability across Caco-2 cells (colonic) can predict *in vivo* (small intestinal) absorption in man—fact or myth. Pharm Res 14:763–766

Živec P, Perdih F, Turel I et al (2012) Different types of copper complexes with the quinolone antimicrobial drugs ofloxacin and norfloxacin: structure, DNA- and albumin-binding. J Inorg Biochem 117:35–47. doi:10.1016/j.jinorgbio.2012.08.008